ENVIRONMENTAL RESEARCH
CLIMATE

PAPER

# Historical catch records of humpback whales and the assessment of early 20th century sea ice edge in climate models

**Marcello Vichi**[1,2,*], **Elisa Seyboth**[3], **Thando Mazomba**[1,9], **Els Vermeulen**[3], **Ken Findlay**[4], **Jan-Olaf Meynecke**[5,6], **Jasper de Bie**[6], **Eduardo Secchi**[7], **Luciano Dalla Rosa**[7] **and Alakendra Roychoudhury**[8]

[1] Department of Oceanography, University of Cape Town, Rondebosch, South Africa
[2] Marine and Antarctic Research centre for Innovation and Sustainability (MARIS), University of Cape Town, Rondebosch, South Africa
[3] Mammal Research Institute Whale Unit, Faculty of Natural and Agricultural Sciences, University of Pretoria, Pretoria, South Africa
[4] Centre for Sustainable Oceans, Cape Peninsula University of Technology, Cape Town, South Africa
[5] Whales and Climate Research Program, Griffith University, Gold Coast, Australia
[6] Centre for Marine and Coastal Research, Griffith University, Gold Coast, Australia
[7] Institute of Oceanography, Federal University of Rio Grande, Rio Grande, Brazil
[8] Department of Earth Sciences, Stellenbosch University, Stellenbosch, South Africa
[9] Now at OceanHub Africa, Cape Town, South Africa.
[*] Author to whom any correspondence should be addressed.

**E-mail:** marcello.vichi@uct.ac.za

**Keywords:** *Megaptera novaeangliae*, Southern Ocean, sea ice, climate model, whaling

Supplementary material for this article is available online

OPEN ACCESS

RECEIVED
10 December 2024

REVISED
23 April 2025

ACCEPTED FOR PUBLICATION
8 May 2025

PUBLISHED
16 May 2025



## Abstract

Assessment of historical environmental conditions in the Southern Ocean is limited by sparse oceanographic records prior to remote-sensing data. Whale catch data, particularly from humpback whales, can help fill this gap, as these whales inhabit waters near the sea ice edge. This study combines historical whale catch data with sea-ice model simulations from CMIP6 to assess the performance in the decade 1930–1939. The models were ranked based on their ability to simulate satellite-observed sea ice seasonality. The high-ranking models locate the sea-ice edge north of historical humpback whale catch regions, indicating higher sea-ice extent at the start of the 20th century, especially in November and December. It is recommended that models be tuned towards these early 20th century conditions while running the pre-industrial simulations. This interdisciplinary approach suggests that using only satellite-era data for model calibration may lead to overestimates of historical sea-ice extent, affecting future predictions.

## 1. Introduction

The future trajectories of Southern Ocean and Antarctic ecosystems are uncertain due to the limited confidence in climate models' ability to accurately replicate the observed high variability of regional Antarctic sea ice (Meredith *et al* 2019). Antarctic sea ice seasonally covers a large portion of the Southern Ocean (Eayrs *et al* 2019), and therefore modulates the exchange of energy between the atmosphere and the ocean, contributing to Earth's overall energy balance (von Schuckmann *et al* 2020). Climate models from the Climate Model Intercomparison Project (Eyring *et al* 2016a) (CMIP, now in phase 6) are the key tools to produce scenario-based future projections of climate conditions and hence of the Antarctic sea ice and its ecosystem response. The reference set of simulations includes the pre-industrial and historical experiments, the latter currently designed to start from 1850 to 2014 (Eyring *et al* 2016a). Bracegirdle *et al* (Bracegirdle *et al* 2015) demonstrated the strong link between the model representation of the observed sea-ice area (SIA) in a climate model and its future projections of temperature, precipitation and SIA. Models that show a bias in the mean sea-ice conditions with respect to the satellite observations tend to retain this bias into the future projections, although there have been clear indications that models may reproduce the right features of 20th

century conditions through error compensation (Hague and Vichi 2018, Holmes *et al* 2019, Li *et al* 2021). Hence, the sea-ice components of climate models are continuously assessed against historical observations over the period of Earth Observations (EO) that started in the late 1970s, either using SIA or sea-ice extent (SIE), which is a more conservative measure that considers the uncertainty of the satellite estimates.

Through the various CMIP analyses, improvements and acceptable skills in the circumpolar SIE seasonal cycle over the EO period have been demonstrated, although the observed historical positive trends are not captured, independently of the model resolution (Maksym 2019, Roach *et al* 2020, Shu *et al* 2020, Selivanova *et al* 2024). These issues are further complicated by the recent shift in the sign of the trend (Purich and Doddridge 2023). Establishing how good models perform in the pre-EO period is however a major challenge because it must be based on proxies and/or correlations with other historical records of atmospheric variables (Maksym 2019, Fogt *et al* 2022). Non-atmospheric sea-ice extent or other edge proxies are particularly not available in summer. De La Mare (de la Mare 1997) used the catch locations from whaling records as a sea ice edge location proxy for the mid 1950s to study the Southern Ocean sea ice edge trends during the age of whaling. The study was broadly criticized for being spatially general in its conclusions, for not considering differences between the different whale species and the foraging conditions, as well as not considering in depth the uncertainties of the satellite data (Vaughan 2000, Ackley *et al* 2003). In a subsequent paper (de la Mare 2009), de La Mare further revisited the proposed approach, but since then there has been no further attempt to reassess the usability of these historical whale catch data. SIE obtained from them has however been used in the literature to compare with climate model results during summertime for the pre-EO period when other proxies are not available (Maksym 2019), indicating how necessary such data are to guide model development and evaluation.

The use of catch data is appealing for multiple reasons linked to the nature of these data. Earlier works focused on the use of all whaling records to extend the duration of the dataset and to allow the reconstruction of trends. There is however a strong merit in restricting the analysis to individual species, especially when they are backed up by the information on their natural habitats. One of the critiques was, for instance, the use of multiple whale data, without any established relationship with the sea ice environment. In particular, Southern Hemisphere humpback whales (*Megaptera novaeangliae*, HW) are known to be found outside the pack ice when compared to other species such as minke whales (*Balaenoptera bonaerensis*) (Ribic *et al* 1991), and whalers did not target whales in consolidated ice conditions. HW are climate-relevant species in the Southern Hemisphere for multiple reasons, including: (1) their longevity and long seasonal migration from low-latitude continental shelves where breeding and calving occur mainly in winter and spring to the high-latitude summer and early autumn feeding grounds (Clapham and Mead 1999), which are typically located between the frontal regions of the Southern Ocean and the ice edge (Meynecke *et al* 2021); and (2) it is a species that underwent an early modern whaling pressure, because this species as the most common to catch using early 20th century whaling techniques (Rocha *et al* 2015). HWs were soon decimated, indicating that information on catches' locations, despite being highly uncertain, is concentrated at the beginning of the historical experiment of the CMIP protocol (Seyboth *et al* 2024).

The aim of this work is to derive information from HW catch data that can be used to refine and constrain climate model simulations of sea-ice conditions at the beginning of the 20th century. We base our analysis on the assumption that such catches, considering their well-documented habitat preferences and historical whaling practices, serve as a reliable proxy for the maximum northward extent of summer ice edge. Our objective is to determine a range of latitudes over which there are plausible reasons to believe that the sea-ice edge was found during the period of maximum exploitation of this species. A corollary question is whether models that perform best in the EO period do well also in the pre-EO period, which would further increase our confidence in their future projections.

## 2. Data and methods

### 2.1. Historical humpback whale catches and sea-ice edges

The International Whaling Commission (IWC) has been compiling information on catch data for all species recorded over time in a Catch Database. Such database is aimed to be as complete and detailed as possible, although there is missing information as records were not done properly, notes were lost over time, etc. It contains known and estimated catch positions for all catches for which such information is available, to the nearest one degree of latitude and longitude possible. However, there are variations in the level of confidence of such position, resulting of the logistics of the operations and the original catch return data provided by that operation (e.g. location, vessel expedition or whaling station). The whaling data used in this work are based on a detailed assessment and review of the historical catch records by Seyboth *et al* (2024). This approach represents an advancement in the catch allocation process by providing the assignment of catches lacking a precise location from the IWC Catch Database (version 5.5), which contains 215 928 HWs' records

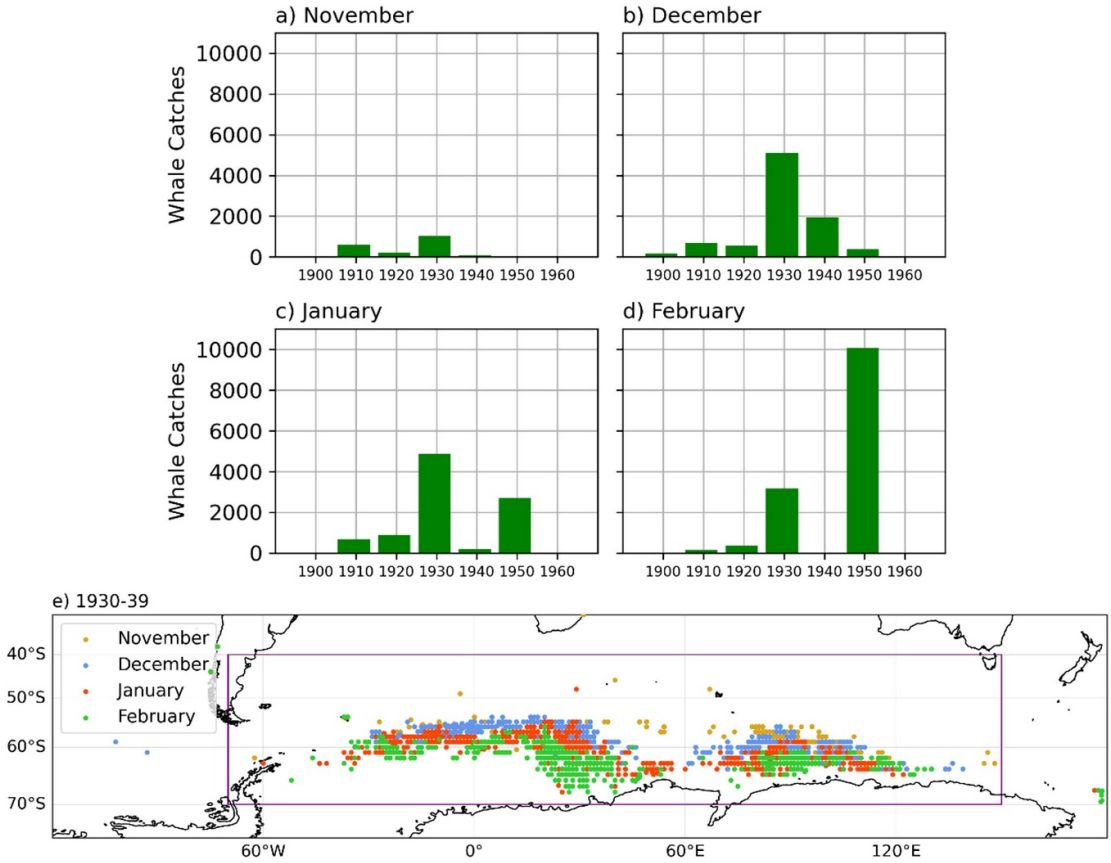


**Figure 1.** (a)–(d) Number of humpback whale catches per decade for each month. (e) Distribution of catches for the 1930–39 decade ($N = 13\,576$). The rectangle indicates the region used in the calculations.

from the Southern Hemisphere in the period 1900–1960 and covers the austral spring-summer months from November to February (Allison 2013). We note that the most recent version 7.1 (Allison 2020) only adds a small number of HW catches, which are located outside of the Southern Ocean. In the Southern Hemisphere, the whaling season ran from mid-October to April and followed the progression of the ice edge (Tønnessen and Johnsen 1982), but very few data are available at the beginning and at the end of the season. We used data from (Seyboth *et al* 2024) to proceed with the analyses, selecting only catches with relatively higher confidence regarding their positions. This means we selected those (i) with known individual locations, (ii) confined to a small area of 10 degrees of latitude by 10 degrees of longitude (e.g. catches identified to the South Shetland Islands or South Georgia), and (iii) with a position estimated based on information of the whaling station operations or moored floating factory. Latitudinal positions were then clustered using 10 degrees longitudinal bins for the statistical analysis. This grid resolution matches the second most detailed level of spatial data available in the IWC Catch Database after individual catch locations (Allison 2020, Seyboth *et al* 2024). We note that latitude is the navigational information that was determined with the highest accuracy by whalers at that time (Tønnessen and Johnsen 1982).

The resulting distribution of catch numbers per month and decade is presented in figure 1. Since the decade 1930–1939 had a consistent number of catches in all the months it was chosen as the reference for the pre-EO period. A total of 13 576 records were used, of which 97.3% had a known position. A poleward shift in the catch locations from November to February is visible, as well as an increase in the latitudinal spread (figure 1(e)). This pattern reinforces the viability of the latitudinal catch data; otherwise, the overlap in the position of the catches would be higher and randomized. In contrast with previous works (de la Mare 1997, 2009), which used the maximum southward catch location and statistically adjusted the latitudinal distribution, we used the median and interquartile ranges of the HW catch latitudinal distributions to estimate the habitat range, considering that HW do not usually enter into the pack ice (Bombosch *et al* 2014, Andrews-Goff *et al* 2018). It is therefore a more conservative estimate of the ice edge location.

Historical locations of the sea-ice edge in the 1930s were compiled in the Discovery Reports (Mackintosh and Herdman 1940, Mackintosh 1972), and have been used in previous studies to compare with whaling data

**Table 1.** CMIP6 models and references used in this study. The models with both the historical and control (pre-industrial) simulations are indicated in column PI. Member r1i1p1f1 was used for every source.

| SOURCE_ID | INSTITUTION_ID | PI | Data References |
|---|---|---|---|
| TaiESM1 | AS-RCEC | * | https://doi.org/10.22033/ESGF/CMIP6.9755. |
| CAS-ESM2-0 | CAS | | https://doi.org/10.22033/ESGF/CMIP6.3353. |
| CanESM5 | CCCma | * | https://doi.org/10.22033/ESGF/CMIP6.3610. |
| CMCC-CM2-HR4 | CMCC | | https://doi.org/10.22033/ESGF/CMIP6.3823. |
| CMCC-CM2-SR5 | CMCC | * | https://doi.org/10.22033/ESGF/CMIP6.3825. |
| CMCC-ESM2 | CMCC | * | https://doi.org/10.22033/ESGF/CMIP6.13195. |
| ACCESS-CM2 | CSIRO-ARCCSS | * | https://doi.org/10.22033/ESGF/CMIP6.4271. |
| ACCESS-ESM1-5 | CSIRO | * | https://doi.org/10.22033/ESGF/CMIP6.4232. |
| EC-Earth3-AerChem | EC-Earth-Consortium | | https://doi.org/10.22033/ESGF/CMIP6.4701. |
| EC-Earth3-CC | EC-Earth-Consortium | * | https://doi.org/10.22033/ESGF/CMIP6.4702. |
| EC-Earth3-Veg-LR | EC-Earth-Consortium | * | https://doi.org/10.22033/ESGF/CMIP6.4707. |
| EC-Earth3-Veg | EC-Earth-Consortium | * | https://doi.org/10.22033/ESGF/CMIP6.4706. |
| EC-Earth3 | EC-Earth-Consortium | * | https://doi.org/10.22033/ESGF/CMIP6.4700. |
| FIO-ESM-2-0 | FIO-QLNM | * | https://doi.org/10.22033/ESGF/CMIP6.9199. |
| MPI-ESM-1-2-HAM | HAMMOZ-Consortium | | https://doi.org/10.22033/ESGF/CMIP6.5016. |
| IPSL-CM5A2-INCA | IPSL | | https://doi.org/10.22033/ESGF/CMIP6.13642. |
| IPSL-CM6A-LR-INCA | IPSL | * | https://doi.org/10.22033/ESGF/CMIP6.13601. |
| IPSL-CM6A-LR | IPSL | * | https://doi.org/10.22033/ESGF/CMIP6.5195. |
| MIROC6 | MIROC | * | https://doi.org/10.22033/ESGF/CMIP6.5603. |
| MPI-ESM1-2-HR | MPI-M | * | https://doi.org/10.22033/ESGF/CMIP6.6594. |
| MPI-ESM1-2-LR | MPI-M | * | https://doi.org/10.22033/ESGF/CMIP6.6595. |
| MRI-ESM2-0 | MRI | * | https://doi.org/10.22033/ESGF/CMIP6.6842. |
| NorCPM1 | NCC | * | https://doi.org/10.22033/ESGF/CMIP6.10894. |
| NorESM2-LM | NCC | | https://doi.org/10.22033/ESGF/CMIP6.8036. |
| NorESM2-MM | NCC | * | https://doi.org/10.22033/ESGF/CMIP6.8040. |
| GFDL-ESM4 | NOAA-GFDL | * | https://doi.org/10.22033/ESGF/CMIP6.8597. |
| SAM0-UNICON | SNU | * | https://doi.org/10.22033/ESGF/CMIP6.7789. |

(Ackley *et al* 2003, de la Mare 2009). We acknowledge that these estimates are subjective reconstructions based on very few data, that they have been digitized from manually compiled maps, and that the inherent uncertainty is unknown. They also do not consider the interannual variability in the decade, because this compilation was based on the composite of locations visited during the expeditions. They are nonetheless an independent indication of the broad location of the sea-ice edge during the period.

### 2.2. Sea-ice extent climatology from remote sensing and climate models

Remotely sensed sea ice concentration (SIC) data for the EO period 1979–2014 were obtained from the OSI-450 Climate Data Record product (Lavergne *et al* 2019). Simulated SIC data from the CMIP6 were obtained from the Pangeo catalogue (Abernathey *et al* 2021, Stern *et al* 2022). Models were selected in terms of their availability of the variables holding SIC and the grid-cell area (*siconc* and *areacello*) for the *historical* experiment (1850–2014), as well as their successful pre-processing using the *xmip* package (Busecke *et al* 2023) on the analysis-ready, cloud optimized (ARCO) data sets. This package does not modify the source data but ensures that all the metadata are consistent and can be used for multi-model analyses. The data processing workflow is available in Vichi (2025). The 26 selected models are listed in table 1 with the corresponding references. Climatological, monthly means of the SIE were calculated from each model using the native grids and then grouped into ensembles for the pre-EO and EO periods (see Data Availability section). A subset of 20 models had valid ARCO data for the *pre-industrial* experiment, and were used to calculate a 100 years ensemble mean. The latitudes of the monthly sea-ice edges from each model were calculated using the 15% SIC threshold and the median and percentiles were calculated to compare with the whaling data.

Models were evaluated according to their skills in reproducing the circumpolar, climatological seasonal cycle of SIE for the EO period (figure 2(a)). The rationale is that models that perform better against the observations are also assumed to have better skills at the beginning of the 20th century. A target diagram (Jolliff *et al* 2009, Rochford 2024) was used to visualise the metrics (figure 2(b)) and separate the mean bias from the unbiased root mean square difference (uRMSD), which quantifies the discrepancy in the seasonal evolution:

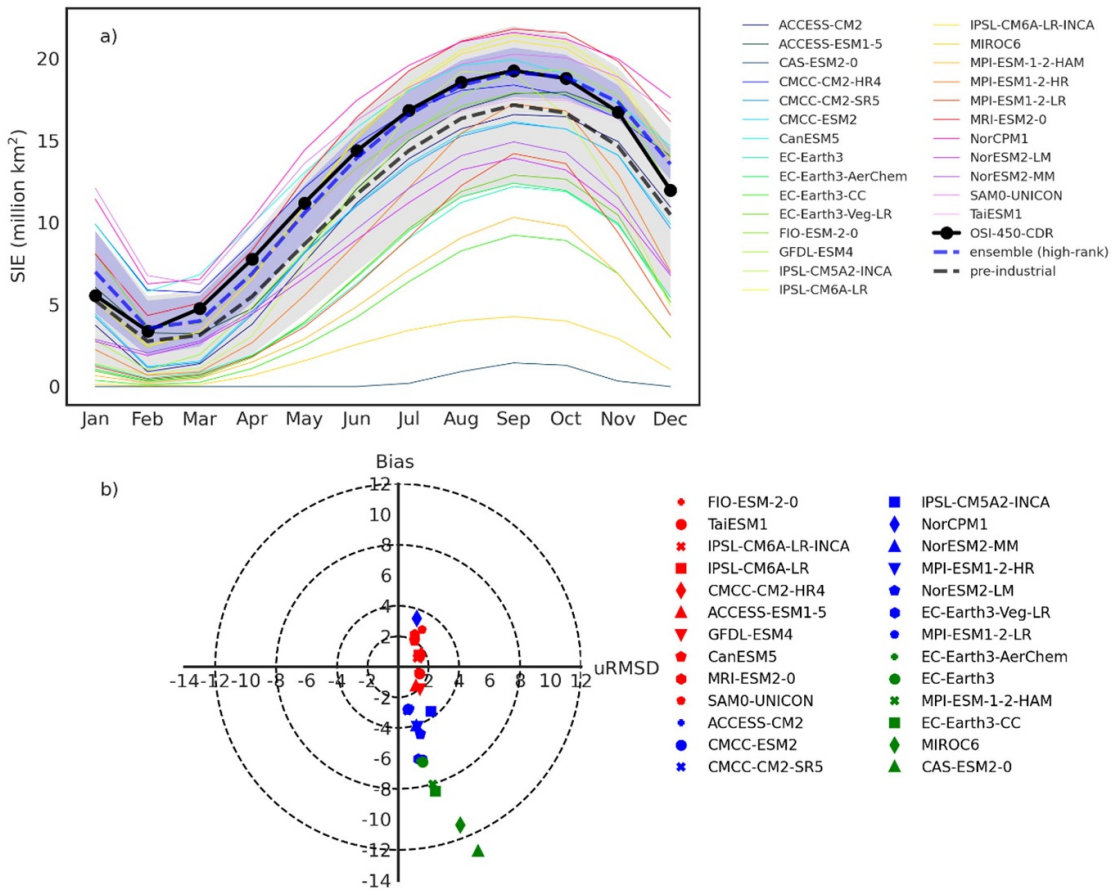


**Figure 2.** (a) Seasonal cycle of Antarctic SIE from the 26 CMIP6 models and the satellite data product, averaged over the EO period. The pre-industrial ensemble mean, and the standard deviation are indicated by the grey dashed line and the shading, respectively. (b) Target diagram showing the mean absolute bias, and the unbiased root mean square difference (uRMSD) (Rochford 2024). The list of models in the legend follows the ranking from the lower to the greater bias; note that the colour coding is not intended to represent the quality, but only to help distinguishing the different models. The ensemble mean and standard deviation obtained by averaging the SIE from the first eight high-ranking models are shown in panel (a) as the blue dashed line and shading.

$$\text{Bias} = \frac{1}{n}\sum_{i=1}^{n}(y_i - x_i)$$

$$\text{uRMSD} = \sqrt{\frac{1}{n}\sum_{i=1}^{n}\left[(x_i - \bar{x}) - (y_i - \bar{y})\right]^2}$$

where $x_i$ are the $n$ monthly reference values and $y_i$ are the corresponding model data, and the overbar symbols represent the means.

Most of the models have a relatively low uRMSD below 2 $10^6$ km$^2$, while only eight models have a bias below this threshold. Models have thus been ranked according to the bias, and the first eight models belong to the high-ranking category, while all the others are classified as low-ranking. The model spread increases from summer to winter, with several models clustering around the seasonal cycle obtained from the OSI-450 product. The ensemble mean of the best models matches the satellite product very closely (figure 2(a)), and the standard deviation is small through all the months. We note that the ensemble mean SIE from the pre-industrial simulation (dashed grey line) is approximately 2 $10^6$ km$^2$ lower than the EO mean in all months but January to March, indicating that SIE was, on average, lower than the historical period although the ensemble spread was larger.

## 3. Results

### 3.1. Simulated summer sea-ice extent over the pre-industrial and historical periods

The simulated SIE pre-EO period in the 1930s corresponding to the HW catches was evaluated against the pre-industrial's and EO period's SIE for the full ensembles and the high-ranking models (figure 3). The

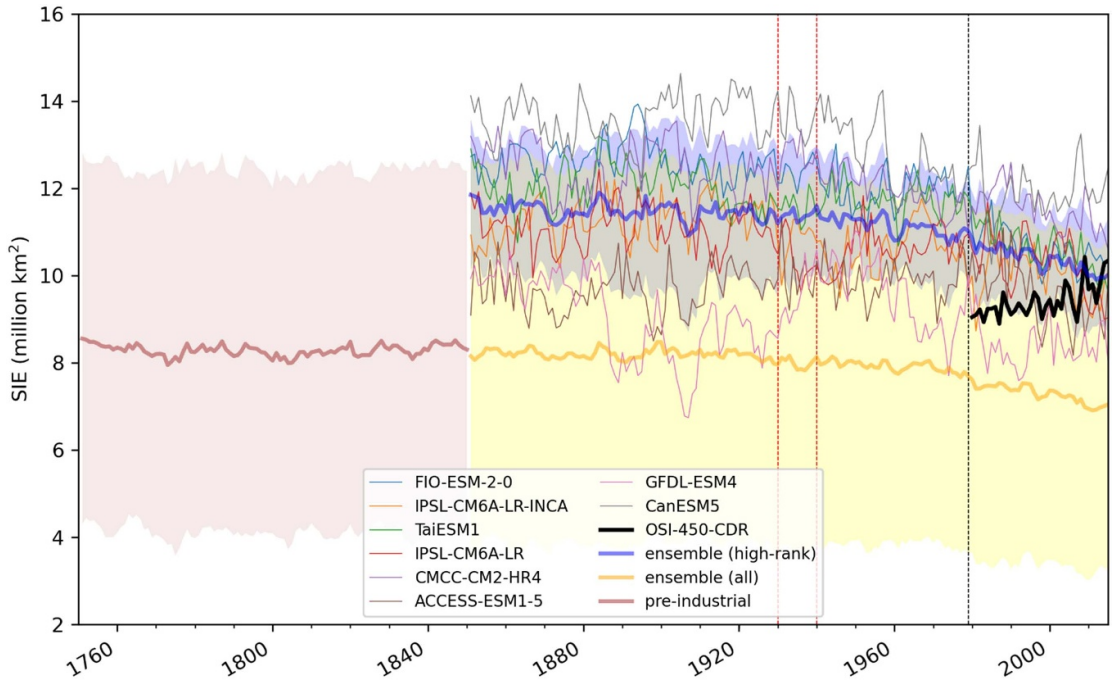


**Figure 3.** Time series of mean SIE from the individual high-ranking models over the whaling season (November–February). Their ensemble mean and standard deviation (in light purple shading) are compared with the historical and pre-industrial means and standard deviations from all the models considered (note that the pre-industrial average from the high-ranking models is not shown since not all the models' data are available). The solid black line represents the mean SIE from the EO satellite data record (1979–2014). The pre-EO and EO periods are shown with the dashed red and black vertical lines, respectively.

pre-industrial ensemble is visibly constant with a large spread, which is maintained throughout the historical experiment (1850–2014). The declining trend analysed in (Roach *et al* 2020) for the CMIP6 simulations of Antarctic sea ice starts around the beginning of the 20th century. It is evident that the models that perform the best against the satellite SIE climatology are located at the higher range of the ensemble's spread. The eight high-ranking models have a wide SIE spread over this period, with an approximated average of $11.5 \pm 1.5\ 10^6\ km^2$.

The observed summer SIE mean is in between the ensemble means of the two groups. Despite the low predictability of the observed positive SIE trend during the EO-period, the ensemble of the best performing models do encompass the trend because about three models show an increase; we also know that the trend from satellite observations has been substantially reverted after 2014 (Purich and Doddridge 2023), aligning more with the model projections. The high-ranking models show the same decreasing trend as the full ensemble, as indicated by the large value of the Pearson correlation coefficient between the two timeseries (0.95).

### 3.2. Ice edge location during the pre-EO period

The comparison of the pre-EO, sea ice edge locations during the whaling season derived from the model ensembles and the statistics of HW catch data from the 1930s is presented in figure 4. We calculated the simulated sea-ice edge using a SIC $> 0\%$ criterion to consider the broadest expansion of ice-covered ocean in the models. The exercise is presented separately for the full ensemble of climate models and for the eight high-ranking models identified in section 2.2. The sea-ice edge from the pre-industrial ensemble is also added to the left column plots. Model statistics are presented with their median and interquartile ranges, while catch data are shown with box-and-whiskers plots and the 'outliers'. The number of data points is different for every longitudinal bin, and some bins are empty, or with too few data to derive a usable distribution. We also note that outliers are simply highlighted because they fall outside of the 5th and 95th percentiles, but they are valid data points in the limits of the historical catch records.

The most prominent feature inferred from the full ensemble in the left columns of figure 4 is the similarity between the pre-industrial and pre-EO sea-ice edge locations. There is an almost complete overlap of the interquartile dispersion, with only minor differences in the medians. The difference between the two ensembles becomes visible only in February in the western region of the Weddell Sea and Antarctic Peninsula, where models in the pre-EO period start showing signs of the declining SIE, with a more southward location of the interquartile range that becomes more evident at the entire circumpolar level later

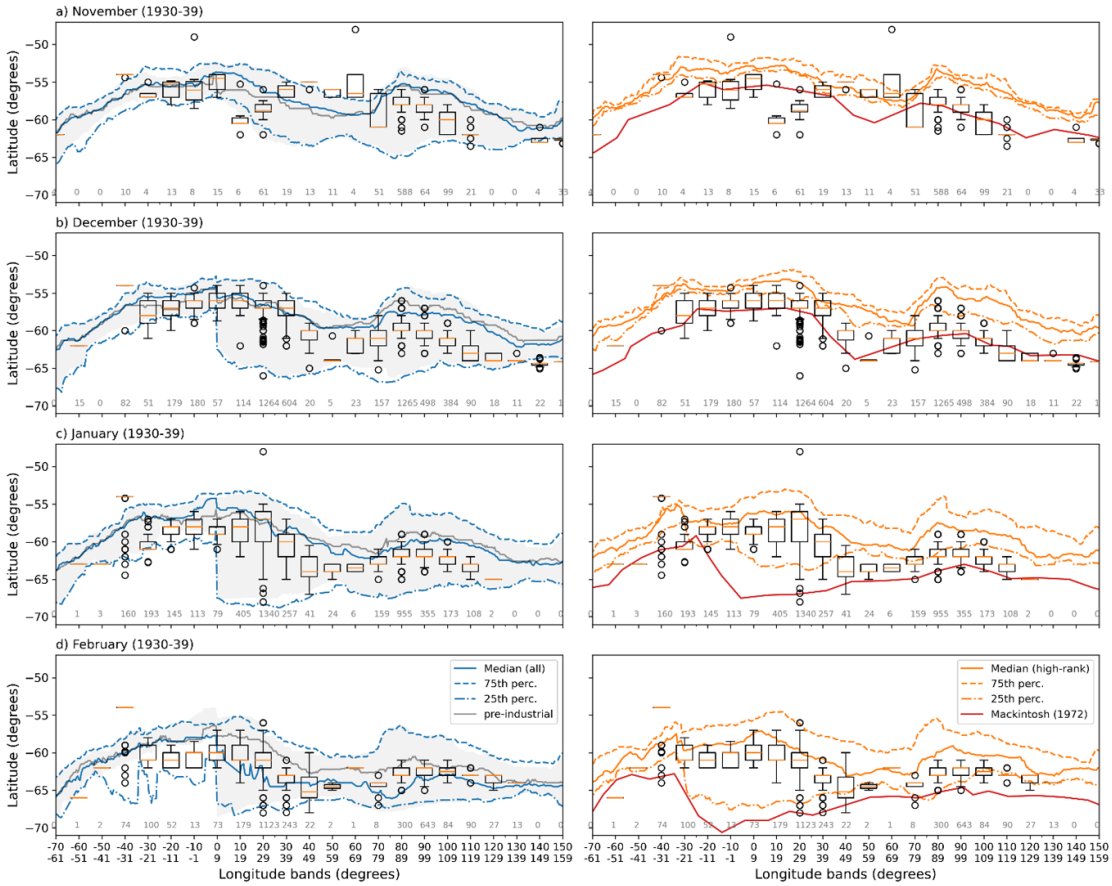


**Figure 4.** Sea-ice edge location over the decade 1930–1939 from the CMIP6 models and from the HW catch data for (a) November, (b) December, (c) January, and (d) February. The median and interquartile range of the 15% concentration contour are shown for all CMIP6 models for the pre-industrial and historical experiments (left column) and for the high-ranking models (right column). The box-and-whiskers represent the median, interquartile range and outliers of the catch latitudes contained within each 10 degrees bin. Number of catches for each bin are shown in grey on the bottom axes. The ice edge location estimated from the Discovery Reports for the 1930s (Mackintosh 1972) is shown in red on the right column plots.

in the historical experiment (figure 3). The distributions of the catch records are within the ranges of the sea-ice edge full ensemble, mostly because the latitudinal dispersion is very high and increases from November to February, almost covering the whole Southern Ocean.

The ice edge median location simulated by the high-ranking models in November and December is shifted equatorward of several degrees compared to the catch data (figures 4(a) and (b), right panels). The interquartile range is narrower than in the full ensembles, and therefore the best performing models show a substantial mismatch with the catch data (figure 2(a)). Despite the anecdotal value of the historical ice edge from the Discovery Reports, it is remarkable to notice the good visual agreement with the catch data distributions in all the months and at most of the longitudes in November and December.

There is an important pattern to highlight in the South Atlantic whaling data between South Georgia and South Africa (40°W—20°E), which is also visible in the spatial map of figure 1(e). The medians of the catches do not shift poleward following the seasonal retreat seen in the simulated and historical ice edges. This implies that the whaling records are found within the larger spread of the modelled sea-ice edge in January and February as also seen in the full ensemble (figures 4(c) and (d)). The alignment of the poleward shifts is instead clearer in Eastern Antarctica (50–120°E). In this sector, the whaling data track the shift of the sea-ice edge, and there is a better agreement with the simulated median from the high-ranking ensemble. The full ensemble contains the whaling data simply because the spread is large, and models disagree on the latitudinal location of the sea-ice edge.

A more quantitative comparison of the sea-ice edge latitudinal differences between whaling data and the simulations of the high-ranking models is presented in figure 5. We calculated the average of the modelled sea-ice edge medians using the same longitudinal bins of the catch data and compared them on a 1–1 plot. Skill score values for each month are shown in the figure legend. Whale catches are consistently located south of the simulated sea-ice edge at almost every longitude and month, with positive mean biases between 1.1–2.1° and large unbiased RMSDs of 4.7–5° latitude. February is the best simulated month from the bias

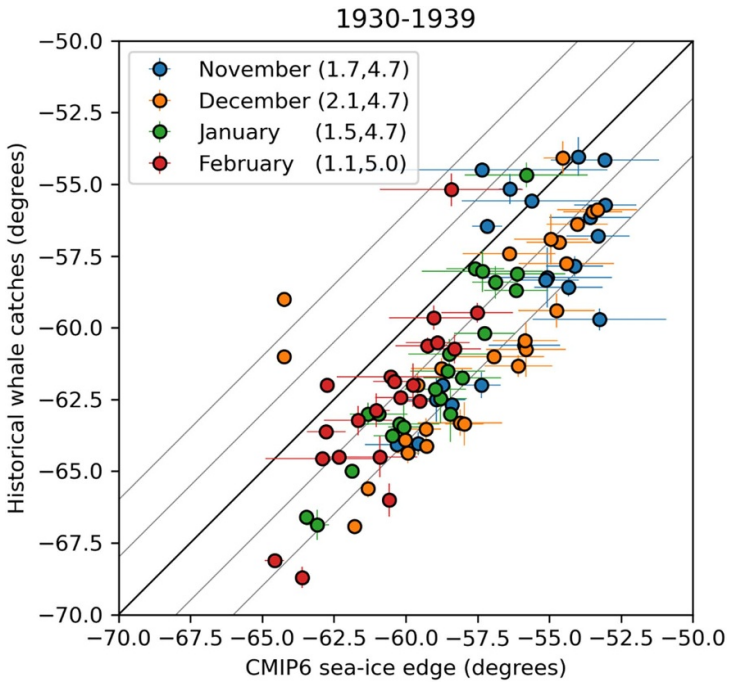


**Figure 5.** Scatter plot of the median latitudes of the sea-ice ice edge location using the 10 degrees bins for the whaling season in the decade 1930–1939. The bars show the standard deviation within the bin, to account for the latitudinal dispersion in certain sectors. The grey lines represent an interval of 2 degrees. The numbers in brackets in the legend are the mean bias and the unbiased root mean square distance for each month. The data are available in the supplementary material.

viewpoint, but the RMSD is the largest, which is more related to the variability in the catch data that are found further away from the ice edge, as highlighted in the previous paragraph.

## 4. Discussion

Whaling catch records carry inherent spatial and temporal uncertainties that have been stressed in the literature when these data were proposed as proxies for sea-ice extent (de la Mare 1997, 2009, Vaughan 2000, Ackley *et al* 2003). Uncertainties on whaling practices and the reporting of catches cannot be quantified further, and we can only rely on historical documents (Seyboth *et al* 2024). On the other hand, proxy data are invaluable for extending the EO period, and when used in the appropriate context they have shown consistency in results and findings (Macalady and Thomas 2017). To overcome the limitations addressed in section 1, we considered the whole distribution of catches' latitudes. We also reassessed these data by restricting them to the species-specific analysis of HW catches, which have been largely decimated in the first decades of the 20th century and are more likely to be a reliable proxy of the early 20th century sea-ice edge location due to the combined habitat preferences and the early exploitation. Blue whales and fin whales became targets after the decimation of HW (Tønnessen and Johnsen 1982), and we assumed that due to the scarcity of prey, the industry was maximizing the efficiency and had similar practices.

CMIP6 simulations were divided into an ensemble of the best performing models (against the climatological seasonal cycle observed from satellites), and the full ensemble of all the available CMIP6 models. This estimation of the edge represents a robust upper boundary; therefore, independently of the remaining uncertainties on catch locations due to our binning methods (see section 2.1), we can make the statement that sea ice was certainly located southward of any HW catch latitude. This concept does not allow us to give an estimate of the SIE, but it can be used more confidently in the assessment process against the modelled edge.

We demonstrated that the distributions of HW catch records in the 1930s spanned more poleward locations than the simulated ensemble median of the sea-ice edge from the high-ranking models. Good skills in reproducing current-climate climatological SIE conditions do not always ensure that trends are properly captured, although models with the best mean state generally show lower biases (e.g. (Roach *et al* 2020, Selivanova *et al* 2024), and the observed trend is contained within the ensemble's range (figure 3). Our results indicate that, in a system characterised by high natural variability like Antarctic sea ice, their mean state representing the early 20th century sea-ice edge can be mislocated. One possible explanation is that a different sea-ice regime was active in the pre-EO period, and that models capturing the EO sea-ice seasonal

cycle fail to represent this state. Fogt *et al* (2022) proposed a SIE reconstruction extending back to 1905 that highlighted a regime shift occurring near 1960. The reconstructed December-February SIE showed no trends in stark contrast with the increase observed in the EO period (figure 3) which may thus be part of multidecadal variability. Our methods cannot be compared directly with a proxy based on SIE, but the model results suggest that, even if there was a regime shift, the high-ranking models show the opposite behaviour because the sea-ice edge location is more equatorward in the pre-EO period than in the last decades. It is beyond the scope of this work to compare the 1930s sea ice edge from whaling records with other proxies or against contemporary conditions. For instance, other proxies such as methansulphonic acid from ice core records (Curran *et al* 2003, Thomas and Abram 2016) are more regional than the distributed whaling records, and they are more adequate for explaining winter conditions.

We notice that the full CMIP6 ensemble encompasses the catches due to the large spread of the interquartile ranges (figure 4). This should not be taken as an indicator of skills, but rather of large model uncertainties in the location of the sea-ice edge during the pre-EO period, especially from December to February. The February sea-ice edge location of the high-ranking model ensemble shows a smaller spread than the full ensemble, and better matches the conditions derived from the catch data, while November indicates the largest overestimation. Given that the seasonal shift of the edge spans an interval of 10 ° latitude during the summer-autumn months, an unbiased RMSD of 5° is of great relevance. The implications for the heat and momentum balance may be important, especially in the marginal ice zone, where the exchanges at the interface are stronger (Vichi 2022). The different biases between early and late summer may be interpreted in two different ways: (1) due to the minimum sea-ice coverage found in February, it is more likely for the high-ranking models that retain more summer SIE to converge towards the estimated pre-EO edge; and (2) the high-ranking climate models have been tuned to match the EO period, resulting in higher autumn-summer SIE in the early 20th century in order to reduce the sea-ice losses and warmer-than-observed sea surface temperature observed in CMIP5 (e.g. (Purich *et al* 2016)).

To explain this point further, we argue that the high-ranking models (but also valid for any other model from the ensemble) may have been indirectly adjusting SIE in the pre-industrial simulation period as part of their tuning practice. A variety of tuning methods are applied in the modelling community (Hourdin *et al* 2017), and a majority of groups use pre-industrial (1850) coupled atmosphere-ocean configurations to adjust the global net top-of-atmosphere flux and then the regional or global mean surface temperatures that are obtained from historical reconstructions (Rayner *et al* 2003). However, model evaluation is generally carried out using essential climate variables from the EO period (Eyring *et al* 2016b). Through this evaluation exercise, the CMIP5 sea surface temperature warm bias in late summer has been attributed to excessive absorbed shortwave radiation (Purich *et al* 2016, Schneider and Reusch 2016). It has been shown that CMIP6 improved on CMIP5, and that biases in SIA against satellite data may be ascribed to thickness biases (Nie *et al* 2023). To achieve this improvement, model parameters in the sea-ice, ocean or atmosphere components may have been adjusted to compensate for the volumetric ice loss to form and maintain a more extended area of thinner ice past wintertime and improve the surface heat budget during summer. The catch data and to some extent the observational historical records from the Discovery Reports (Mackintosh 1972) suggest that sea-ice edge was instead found more poleward during the whaling period, and this information should be used when tuning the pre-industrial simulations.

However, the Atlantic sector between South Georgia and South Africa deserves a specific discussion, because it appears less likely that HW catches (or any other whaling data) can be used as a sea-ice proxy in this region. HW catch records are within the interquartile range of the sea ice edge location from the high-ranking models for January and February, but the Discovery Reports are more poleward, as the spread of models from the ensemble suggest (first column in figure 4). Whales were caught more equatorward, with a much larger latitudinal spread, in line with the contemporary distribution of krill (Atkinson *et al* 2008, El-Gabbas *et al* 2021, Bamford *et al* 2022). Due to the features of the Antarctic Circumpolar Current, the feeding grounds in this region are at higher latitudes compared to other regions such as Eastern Antarctica (Meynecke *et al* 2021, Seyboth *et al* 2024). The number of catches is in fact consistently high in this sector (figure 4), especially in December and January. According to the whaling data alone, there is no strong indication that HW would necessarily move closer to the ice edge for feeding in late summer. Considering this caveat, there is some confidence that the CMIP6 model ensemble has a reasonable representation of the late summer conditions at the beginning of the century in this region despite the catches telling a different story.

On the other hand, there is strong evidence that the east Antarctic sea-ice edge was much further south than simulated by the high-performing models. The median of the full ensemble is a better descriptor for HW catches in the western sector of the Indian Ocean between 30°–50°E. Given that this sector holds a good number of catches in the database, and that the southern feeding areas in East Antarctica were largely unknown until the illegal catch histories of the Soviet fleets from the 1950s were published (Rocha *et al*

2015), it is likely that the ice edge was indeed poleward in January and February, as also suggested by the Discovery records. The whaling records are therefore a useful proxy for model evaluation in this sector.

## 5. Conclusions

The whaling era represented a dark age for the Southern Ocean ecosystem, and the HW populations are now recovering differently in different sectors (Seyboth *et al* 2023), while being exposed to a continuously changing climate (Meynecke *et al* 2020). Whaling records are very valuable, and they must be used with caution and with careful consideration of the context. A good understanding of the catch data is essential (Seyboth *et al* 2024), as well as interdisciplinary collaborations between whale experts and climate modellers. We propose a metrics for climate model assessment based on these data, but we also caution about the use of these data for estimating absolute values of the SIE. There are very few data to constrain pre-industrial simulations; given the general similarity between this pre-EO reference period and the last 100 years of the pre-industrial experiments, it is recommended that these data be used as a further set of evaluation data for the pre-industrial tuning of climate models, to ensure an adequate inclusion of sea ice as a regulator of the heat and momentum exchanges in the pre-industrial Southern Ocean.

## Data availability statement

All the CMIP6 data are available in the cloud catalogue maintained by Pangeo Forge (https://pangeo-forge.readthedocs.io, accessed on 10/12/2024). The International Whaling Commission Individual Catch Database is available upon request to the IWC (Allison 2013, 2020). The Python notebooks used to process the data and generate the figures are available in Vichi (2025).

The data that supports the findings of this study are openly available in the supplementary files of this article.

## Acknowledgment

This work was supported by an anonymous private donation to the Whales & Climate Research Program (https://whalesandclimate.org). We are grateful to the World Climate Research Programme's Working Group on Coupled Modelling and the CMIP modelling groups that made available their model output through the Earth System Grid Federation (ESGF), and to the International Whaling Commission for the access to the Catch Database. We are indebted to the Pangeo community for proposing and implementing the cloud-ready version of the ESGF dataset, which substantially improved the capability to analyse the climate model data. The authors wish to thank Prof M E J Lopez and the whole team at the Whales & Climate Research Program for their contributions.

## ORCID iDs

Marcello Vichi https://orcid.org/0000-0002-0686-9634
Elisa Seyboth https://orcid.org/0000-0002-1506-0861
Thando Mazomba https://orcid.org/0000-0001-6829-9887
Els Vermeulen https://orcid.org/0000-0002-3667-1290
Ken Findlay https://orcid.org/0000-0001-7154-8805
Jan-Olaf Meynecke https://orcid.org/0000-0002-4639-4055
Jasper de Bie https://orcid.org/0000-0002-8371-4089
Alakendra Roychoudhury https://orcid.org/0000-0002-5627-8891

## References

Abernathey R P *et al* 2021 Cloud-native repositories for big scientific data *Comput. Sci. Eng.* **23** 26–35
Ackley S, Wadhams P, Comiso J C and Worby A P 2003 Decadal decrease of Antarctic sea ice extent inferred from whaling records revisited on the basis of historical and modern sea ice records *Polar Res.* **22** 19–25
Allison C 2013 IWC individual large whale catch database. Version 5.5. Available from the international whaling commission, 135 Station Road, Impington, Cambridge, CB24 9NP UK. [statistics@iwc.int] (International Whaling Commission)
Allison C 2020 IWC individual large whale catch database. Version 7.1. Available from the international whaling commission, 135 Station Road, Impington, Cambridge, CB24 9NP UK. [statistics@iwc.int] (International Whaling Commission)
Andrews-Goff V, Bestley S, Gales N J, Laverick S M, Paton D, Polanowski A M, Schmitt N T and Double M C 2018 Humpback whale migrations to Antarctic summer foraging grounds through the southwest Pacific Ocean *Sci. Rep.* **8** 12333
Atkinson A *et al* 2008 Oceanic circumpolar habitats of Antarctic krill *Mar. Ecol. Prog. Ser.* **362** 1–23

Bamford C C G, Jackson J A, Kennedy A K, Trathan P N, Staniland I J, Andriolo A, Bedriñana-Romano L, Carroll E L, Martin S and Zerbini A N 2022 Humpback whale (*Megaptera novaeangliae*) distribution and movements in the vicinity of South Georgia and the South sandwich islands marine protected area *Deep Sea Res. II* **198** 105074
Bombosch A, Zitterbart D P, Van Opzeeland I, Frickenhaus S, Burkhardt E, Wisz M S and Boebel O 2014 Predictive habitat modelling of humpback (Megaptera novaeangliae) and Antarctic minke (Balaenoptera bonaerensis) whales in the Southern Ocean as a planning tool for seismic surveys *Deep Sea Res. I* **91** 101–14
Bracegirdle T J, Stephenson D B, Turner J and Phillips T 2015 The importance of sea ice area biases in 21st century multimodel projections of Antarctic temperature and precipitation *Geophys. Res. Lett.* **42** 10–832
Busecke J, Ritschel M, Maroon E and Nicholas T 2023 xMIP: v0.7.1 software (https://doi.org/10.5281/zenodo.7519179)
Clapham P J and Mead J G 1999 Megaptera novaeangliae *Mamm. Species* **604** 1–9
Curran M A J, van Ommen T D, Morgan V I, Phillips K L and Palmer A S 2003 Ice core evidence for Antarctic sea ice decline since the 1950s *Science* **302** 1203–6
de la Mare W K 1997 Abrupt mid-twentieth-century decline in Antarctic sea-ice extent from whaling records *Nature* **389** 57–60
de la Mare W K 2009 Changes in Antarctic sea-ice extent from direct historical observations and whaling records *Clim. Change* **92** 461–93
Eayrs C, Holland D, Francis D, Wagner T, Kumar R and Li X 2019 Understanding the seasonal cycle of Antarctic sea ice extent in the context of longer-term variability *Rev. Geophys.* **57** 1037–64
El-Gabbas A, Van Opzeeland I, Burkhardt E and Boebel O 2021 Static species distribution models in the marine realm: the case of baleen whales in the Southern Ocean *Divers. Distrib.* **27** 1536–52
Eyring V *et al* 2016b ESMValTool (v1.0)—a community diagnostic and performance metrics tool for routine evaluation of Earth system models in CMIP *Geosci. Model Dev.* **9** 1747–802
Eyring V, Bony S, Meehl G A, Senior C A, Stevens B, Stouffer R J and Taylor K E 2016a Overview of the coupled model intercomparison project phase 6 (CMIP6) experimental design and organization *Geosci. Model Dev.* **9** 1937–58
Fogt R L, Sleinkofer A M, Raphael M N and Handcock M S 2022 A regime shift in seasonal total Antarctic sea ice extent in the twentieth century *Nat. Clim. Change* **12** 54–62
Hague M and Vichi M 2018 A link between CMIP5 phytoplankton phenology and sea ice in the Atlantic Southern Ocean *Geophys. Res. Lett.* **45** 6566–75
Holmes C R, Holland P R and Bracegirdle T J 2019 Compensating biases and a noteworthy success in the CMIP5 representation of Antarctic sea ice processes *Geophys. Res. Lett.* **46** 4299–307
Hourdin F *et al* 2017 The art and science of climate model tuning *Bull. Am. Meteorol. Soc.* **98** 589–602
Jolliff J K, Kindle J C, Shulman I, Penta B, Friedrichs M A M, Helber R and Arnone R A 2009 Summary diagrams for coupled hydrodynamic-ecosystem model skill assessment *J. Mar. Syst.* **76** 64–82
Lavergne T *et al* 2019 Version 2 of the EUMETSAT OSI SAF and ESA CCI sea-ice concentration climate data records *Cryosphere* **13** 49–78
Li S, Huang G, Li X, Liu J and Fan G 2021 An assessment of the Antarctic sea ice mass budget simulation in CMIP6 historical experiment *Front. Earth Sci.* **9** 649743
Macalady A and Thomas K (ed) 2017 Antarctic sea ice variability in the Southern Ocean-climate system *Proc. a Workshop* (*Washington, D.C*) (National Academies Press) (https://doi.org/10.17226/24696)
Mackintosh N A 1972 Life cycle of Antarctic krill in relation to ice and water conditions, discovery reports (Discovery Reports)
Mackintosh N A and Herdman H F P 1940 Distribution of the pack-ice in the Southern Ocean, discovery reports (Discovery Reports)
Maksym T 2019 Arctic and Antarctic sea ice change: contrasts, commonalities, and causes *Annu. Rev. Mar. Sci.* **11** 187–213
Meredith M *et al* 2019 Polar regions *IPCC Special Report on the Ocean and Cryosphere in a Changing Climate* (Cambridge University Press) pp 203–320
Meynecke J-O *et al* 2020 Responses of humpback whales to a changing climate in the Southern Hemisphere: priorities for research efforts *Mar. Ecol.* **41** e12616
Meynecke J-O *et al* 2021 The role of environmental drivers in humpback whale distribution, movement and behavior: a review *Front. Mar. Sci.* **8** 1685
Nie Y, Lin X, Yang Q, Liu J, Chen D and Uotila P 2023 Differences between the CMIP5 and CMIP6 Antarctic sea ice concentration budgets *Geophys. Res. Lett.* **50** e2023GL105265
Purich A, Cai W, England M H and Cowan T 2016 Evidence for link between modelled trends in Antarctic sea ice and underestimated westerly wind changes *Nat. Commun.* **7** 10409
Purich A and Doddridge E W 2023 Record low Antarctic sea ice coverage indicates a new sea ice state *Commun. Earth Environ.* **4** 1–9
Rayner N A, Parker D E, Horton E B, Folland C K, Alexander L V, Rowell D P, Kent E C and Kaplan A 2003 Global analyses of sea surface temperature, sea ice, and night marine air temperature since the late nineteenth century *J. Geophys. Res.* **108** 4407
Ribic C A, Ainley D G and Fraser W R 1991 Habitat selection by marine mammals in the marginal ice zone *Antarct. Sci.* **3** 181–6
Roach L A *et al* 2020 Antarctic Sea Ice Area in CMIP6 *Geophys. Res. Lett.* **47** e2019GL086729
Rocha R C Jr, Clapham P J and Ivashchenko Y 2015 Emptying the oceans: a summary of industrial whaling catches in the 20th century *Mar. Fish. Rev.* **76** 37–48
Rochford P 2024 SkillMetrics, software (https://doi.org/10.5664/jcsm.11128)
Schneider D P and Reusch D B 2016 Antarctic and Southern Ocean surface temperatures in CMIP5 models in the context of the surface energy budget *J. Clim.* **29** 1689–716
Selivanova J, Iovino D and Vichi M 2024 Limited benefits of increased spatial resolution for sea ice in HighResMIP simulations *Geophys. Res. Lett.* **51** e2023GL107969
Seyboth E, Meynecke J-O, de Bie J, Roychoudhury A and Findlay K 2023 A review of post-whaling abundance, trends, changes in distribution and migration patterns, and supplementary feeding of Southern Hemisphere humpback whales *Front. Mar. Sci.* **10** 997491
Seyboth E, Paarman S, Allison C, Meynecke J-O, de Bie J and Findlay K P 2024 A review of Southern Hemisphere humpback whaling by period and catch location *J. Cetacean Res. Manage.* **25** 123–62
Shu Q, Wang Q, Song Z, Qiao F, Zhao J, Chu M and Li X 2020 Assessment of sea ice extent in CMIP6 with comparison to observations and CMIP5 *Geophys. Res. Lett.* **47** e2020GL087965
Stern C, Abernathey R, Hamman J, Wegener R, Lepore C, Harkins S and Merose A 2022 Pangeo forge: crowdsourcing analysis-ready, cloud optimized data production *Front. Clim.* **3** 782909

Thomas E R and Abram N J 2016 Ice core reconstruction of sea ice change in the Amundsen-Ross Seas since 1702 A.D *Geophys. Res. Lett.* **43** 5309–17
Tønnessen J N and Johnsen A O 1982 *The History of Modern Whaling* (University of California Press)
Vaughan S 2000 Can Antarctic sea-ice extent be determined from whaling records? *Polar Rec.* **36** 345–7
Vichi M 2022 An indicator of sea ice variability for the Antarctic marginal ice zone *Cryosphere* **16** 4087–106
Vichi M 2025 Whales-CMIP6, software (https://doi.org/10.25375/uct.28827347)
von Schuckmann K *et al* 2020 Heat stored in the Earth system: where does the energy go? *Earth Syst. Sci. Data* **12** 2013–41